THE JOURNAL OF BIOLOGICAL CHEMISTRY VOL. 288, NO. 35, pp. 25414–25427, August 30, 2013

MicroRNA-124 Suppresses the Transactivation of Nuclear Factor of Activated T Cells by Targeting Multiple Genes and Inhibits the Proliferation of Pulmonary Artery Smooth Muscle Cells*

Received for publication, February 8, 2013, and in revised form, July 9, 2013 Published, JBC Papers in Press, July 12, 2013, DOI 10.1074/jbc.M113.460287

Kang Kang[‡1], Xiao Peng[‡1], Xiaoying Zhang[‡], Yuna Wang[‡], Lishu Zhang[§], Li Gao[§], Tingting Weng[§], Honghao Zhang[§], Ramaswamy Ramchandran[¶], J. Usha Raj[¶], Deming Gou[‡§¶2], and Lin Liu[§3]

From the [‡]College of Life Sciences, Shenzhen Key Laboratory of Microbial Genetic Engineering, Shenzhen University, Shenzhen, Guangdong 518060, China, the [§]Department of Physiological Sciences, Oklahoma State University, Stillwater, Oklahoma 74078, and the [¶]Department of Pediatrics, University of Illinois, Chicago, Illinois 60612

Background: The NFAT signaling pathway is linked to pulmonary arterial hypertension.
Results: MicroRNA screening revealed that miR-124 robustly inhibits NFAT activity, dephosphorylation, and nuclear translocation of NFAT by targeting multiple genes, NFATc1, CAMTA1, and PTBP1.
Conclusion: miR-124 is an effective and multipronged inhibitor of NFAT signaling.
Significance: miR-124 might be a potential immunosuppressant that may have biological effects linked to pulmonary arterial hypertension.

Abnormal proliferation and phenotypic modulation of pulmonary artery smooth muscle cells (PASMC) contributes to the pathogenesis of numerous cardiovascular disorders, including pulmonary arterial hypertension (PAH). The nuclear factor of activated T cells (NFAT) signaling pathway is linked to PASMC proliferation and PAH. MicroRNAs (miRNAs) are small noncoding RNAs that function in diverse biological processes. To systemically identify the specific miRNAs that regulate the NFAT pathway, a human primary miRNA library was applied for cell-based high throughput screening with the NFAT luciferase reporter system. Eight miRNAs were found to modulate NFAT activity efficiently. Of them, miR-124 robustly inhibited NFAT reporter activity and decreased both the dephosphorylation and the nuclear translocation of NFAT. miR-124 also inhibited NFAT-dependent transcription of IL-2 in Jurkat T cells. miR-124 exerted its effects by targeting multiple genes, including a known component of the NFAT pathway, NFATc1, and two new regulators of NFAT signaling, CAMTA1 (calmodulin-binding transcription activator 1) and PTBP1 (polypyrimidine tract-binding protein 1). Physiologically, miR-124 was down-regulated by hypoxia in human PASMC, consistent with the activation of NFAT during this process. Down-regulation of miR-124 was also observed in 3-week hypoxia-treated mouse lungs. Furthermore, the overexpression of miR-124 not only inhibited human PASMC proliferation but also maintained its differentiated phenotype by repressing the NFAT pathway. Taken together, our data provide the first evidence that miR-124 acts as an inhibitor of the NFAT pathway. Down-regulation of miR-124 in hypoxia-treated PASMC and its antiproliferative and prodifferentiation effects imply a potential value for miR-124 in the treatment of PAH.

The nuclear factor of activated T cells (NFAT),[4] originally identified in T lymphocytes, represents a family of Ca^{2+}-dependent transcription factors comprising four well characterized isoforms, NFATc1 to -c4 (1–3). In resting cells, the phosphorylated NFAT remains in the cytoplasm in an inactive form. Dephosphorylation of NFAT by calcineurin, a Ca^{2+}/calmodulin-dependent phosphatase, unmasks nuclear localization signals and results in its translocation from the cytoplasm into the nucleus, where it binds cognate DNA motifs at enhancer sites and regulates gene transcription (3). Functionally, it has become increasingly clear that NFAT is operative not only in T cells but also in other type of cells and regulates numerous developmental programs in vertebrates (4).

Pulmonary arterial hypertension (PAH) is a devastating, life-threatening disorder characterized by elevated pulmonary vascular resistance and pulmonary arterial pressure (5, 6).

* This work was supported by National Natural Science Foundation of China Grant 81170047 (to D. G.), National Basic Research Program of China 973 Program Grant 2012CB124701, Shenzhen Overseas High Level Talents Innovation Program Grant YFZZ20111009 (to D. G.), Shenzhen Municipal Basic Research Program Grant JC201006010725A (to D. G.), American Heart Association Grant-in-aid 0865162F (to D. G.), and National Institutes of Health Grants R01 HL083188, R01 HL071628, and R01 HL052146 (to L. L.) and R01 HL075187 (to J. U. R.) from NHLBI.
[1] Both authors contributed equally to this work.
[2] To whom correspondence may be addressed: College of Life Sciences, Shenzhen University, Nanhai Ave. 3688, Shenzhen, Guangdong 518060, China. Tel.: 86-755-26527848; Fax: 86-755-26534274; E-mail: dmgou@szu.edu.cn.
[3] To whom correspondence may be addressed: Dept. of Physiological Sciences, Oklahoma State University, 264 McElroy Hall, Stillwater, OK 74078. Tel.: 405-744-4526; Fax: 405-744-8263; E-mail: lin.liu@okstate.edu.

[4] The abbreviations used are: NFAT, nuclear factor of activated T cells; PASMC, pulmonary artery smooth muscle cell(s); HPASMC, human pulmonary artery smooth muscle cell(s); PAH, pulmonary arterial hypertension; miRNA, microRNA; SMC, smooth muscle cell(s); α-SMA, α-smooth muscle actin; PMA, phorbol 12-myristate 13-acetate; qRT-PCR, quantitative RT-PCR; EGFP, enhanced green fluorescent protein.

Although the specific mechanisms responsible for the development of PAH remain unknown, abnormal proliferation and phenotypic switching of pulmonary artery smooth muscle cells (PASMC) from a contractile, differentiated phenotype to a synthetic, undifferentiated phenotype is an early event in this disease (7–9). A number of factors play roles in the abnormal proliferation of PASMC, and hypoxia is one of the important stimuli. Several recent observations suggest that NFAT family members are involved in the development of PAH. NFATc2 has been shown to be up-regulated and activated in PAH patients (10). Also, in a mouse model of PAH, chronic hypoxia induces the expression and activation of NFATc3, which may contribute to pulmonary hypertension and vascular remodeling (11, 12). Intriguingly, NFAT is also activated in hypoxia-treated human PASMC (HPASMC) or the HPASMC isolated from PAH patients, which is associated with increased cell proliferation and resistance to apoptosis (13). Conversely, the inhibition of NFAT by VIVIT (a competitive peptide that inhibits the docking of NFAT to calcineurin) or cyclosporin A (an inhibitor of calcineurin) suppresses hypoxia-induced proliferation and leads to increased apoptosis of PASMC *in vitro* (14). These findings support an important role for NFAT-mediated signaling in the pathogenesis of PAH.

MicroRNAs (miRNAs) are a class of small non-coding RNA molecules that post-transcriptionally down-regulate gene expression by binding to the 3′-untranslated region (UTR) of specific mRNA targets (15, 16). Recent studies have revealed the importance of miRNAs in the development of PAH. miR-143 and miR-145 are enriched in vascular smooth muscle cells (SMC) and play an essential role in controlling the phenotypic switch of SMC during vascular diseases (17–19). The extent of miR-204 down-regulation correlates with PAH severity and accounts for the proliferative and antiapoptotic phenotypes of PAH-PASMC. Delivery of synthetic miR-204 into the lungs of PAH rats significantly reduced disease severity (20). Our previous study has demonstrated the role of miR-21 in hypoxia-mediated HPASMC proliferation and migration (21). Recently, we found that miR-210, a major hypoxia-induced miRNA, exerts an antiapoptotic effect and may contribute to the development of PAH (22).

Although accumulating data have suggested that miRNAs function in regulating SMC proliferation and differentiation (23–25), whether this effect is achieved by regulating NFAT signaling pathway through miRNAs is still unclear. In this study, we performed a high throughput screening by using an in-house-made miRNA expression library and NFAT luciferase reporter system. We identified eight miRNAs that modulate NFAT activity with at least 2-fold change. Among them, miR-124 robustly suppressed NFAT activity and decreased both the dephosphorylation and the nuclear translocation of NFAT by targeting multiple genes. Functionally, miR-124, which is down-regulated in both hypoxia-treated HPASMC and chronic hypoxia-induced PAH mouse lungs, had both antiproliferative and prodifferentiation roles. Our studies suggest that miR-124 might be a potential target in PAH therapy via its inhibition of NFAT signaling.

MATERIALS AND METHODS

Cell Culture—Human 293A, 293T, Jurkat T, and U2-OS cells were purchased from the American Type Culture Collection (Manassas, VA) and maintained in Dulbecco's modified Eagle's medium (DMEM) supplemented with 10% fetal bovine serum. HPASMC (Lonza, Walkersville, MD) were cultured in SmGM-2 smooth muscle cell growth medium (Lonza). The medium for HPASMC was changed every other day. Hypoxia treatment of HPASMC was done in a special hypoxia incubator (Forma 3130, Thermo Scientific) infused with a gas mixture of 5% CO_2, balance nitrogen to obtain ~3% oxygen concentration.

PAH Mouse Model—Chronic hypoxia-induced PAH in a mouse model was developed as described previously (22). The expression level of miR-124 was analyzed by quantitative PCR using total RNA extracted from normoxia- and hypoxia-exposed mouse lungs. snoRNA-202 was used as an internal control for normalization.

miRNA Expression Library and Plasmids—Approximately 300 primary miRNAs (~0.5 kb long) were PCR-amplified from human genomic DNA and cloned after the EGFP stop codon in the pENTR/CMV-EGFP and/or pFIV/CMV-EGFP vector named pENTR/CMV-EGFP-miRNA or pFIV/CMV-EGFP-miRNA. Human Ubc (ubiquitin C) promoter-driven miR-124a-2 overexpression vector (pUbc/miR124a-2) was generated by replacing the CMV-EGFP fragment in pENTR/CMV-EGFP-miR124a-2 vector with the Ubc promoter, which was amplified from pL-UGIP vector (Sigma). The pUbc/Control without miRNA insert was also constructed and used as a negative control vector.

To construct GFP-tagged NFATc1 expression vector, NFATc1 cDNA with the complete coding region and its 3′-UTR was PCR-amplified from a mouse NFATc1 cDNA clone (IMAGE: 5354603) using the forward primer 5′-CACCTCGAGCAATGCCAAGTACCAGCTT-3′ and reverse primer 5′-GAGAATTCACTGCTTTATTGGATTCATC-3′ and cloned into pAcGFP-C1 vector (Clontech) through XhoI/EcoRI sites, resulting in pAcGFP-NFATc1-UTR. pAcGFP-NFATc1 vector without the NFATc1 3′-UTR was constructed by inserting the NFATc1 coding region, which was obtained by PCR amplification with the same forward primer and a new reverse primer (5′-GA***GAATTC***AGTTACTGCGGCTGTAGCCT-3′). We also constructed lentiviral vectors to express three different NFATs (NFATc1, -c2, and -c3). NFATc1 cDNA fragment released from pAcGFP-NFATc1 vector by XhoI-EcoRI was subcloned into pLVX-puro vector (Clontech), resulting in pLVX-NFATc1. NFATc2 cDNA fragment with an N-terminal c-Myc tag was PCR-amplified from a mouse NFATc2 plasmid (plasmid 11791, ordered from Addgene) using the forward primer containing the c-Myc tag 5′-CACC**GGTCTC**GTCGACCACCATGGAGCAAAAGCTCATTTCTGAAGAGGACCTCTCTCGAGCAATGGACGTCCCGGAGCCGCAG-3′ and the reverse primer 5′-CACC**GGTCTC**GAATTCTAGGTCTGATTTCGGGAGGGAGGTCCTGA-3′ (EcoR31I in boldface type) and cloned into pLVX-puro vector through XhoI-EcoRI sites, resulting in pLVX-cMyc-NFATc2. The NFATc3 cDNA fragment was PCR-amplified from human NFATc3 cDNA clone vector (IMAGE: 100009844, ordered from Open

Biosystems) using the forward primer 5′-CAC**CTCGAG**CAATGACTACTGCAAACTG-3′ and the reverse primer 5′-GA**GAATTC**AGTTAGAGCCCATCAGATC-3′ and cloned into pLVX-puro vector through XhoI-EcoRI sites, generating a new vector of pLVX-NFATc3.

The human U6 promoter-driven RNAi vector was previously generated in our laboratory (26). The siRNA sequences against their targets are listed in Table 1. Most of them were selected from published reports with validated silencing efficiency. Short hairpin shRNA inserts from two annealed oligonucleotides were cloned into pENTR/U6 vector through BamHI-XhoI restriction sites. All of the constructs were confirmed by DNA sequencing.

Lentivirus Package and Infection—High titer lentivirus was packaged in 293T cells by co-transfecting a lentiviral vector and Lenti-X HT packaging plasmids (Clontech) with jetPEI® DNA transfection reagent (Polyplus Transfection, New York, NY). The same amounts of lentivirus were used to infect HPASMC cultured in 60-mm dishes in the presence of Polybrene (4 μg/ml).

NFAT-responsive Luciferase Reporter Assay—To screen the miRNAs that regulate NFAT activity, an NFAT reporter assay was carried out in 293A cells using NFAT reporter vector (pGL4.30[luc2P/NFAT-RE/Hygro]) and normalization control vector (phRL-TK) (Promega, Madison, WI). Briefly, 293A cells (1×10^4) were added into each well and cultured overnight. The cells were transfected with a DNA mixture containing 25 ng of pGL4.30, 2.5 ng of phRL-TK, and 75 ng of miRNA expression vector using Lipofectamine 2000 (Invitrogen). After a 32-h transfection, cells were stimulated with PMA (10 ng/ml) and ionomycin (1 μM) for 18 h and then harvested for the luciferase assay using the Dual-Luciferase® reporter assay system (Promega). Cells without stimulation were also included. For each assay, the initial screen was run in duplicate. Compared with the EGFP control vector, miRNAs that changed the NFAT reporter activity greater than or less than 2-fold were selected and subsequently reassayed on 24-well plates. To further exclude the possibility that the miRNAs could be a global activator/inactivator of transcription, the Dual-Luciferase assay was also performed with the backbone reporter plasmid, pGL4.27, which does not contain the NFAT response element in pGL4.3 vector.

Target Prediction and Verification—We applied the TargetScan algorithm to predict targets of miRNAs and then verified them by a 3′-UTR reporter assay. The 3′-UTRs of predicted target genes were PCR-amplified and inserted into a modified pGL3 control vector through EcoRI-XbaI restriction sites, resulting in pFLuc-3′UTR. NFATc1 3′-UTR was amplified with the primer pairs 5′-GAGAATTCATACGTAACGACCTC-3′ and 5′-GGATCTAGAACTGCTTTATTGGATTCATCTC-3′ using mouse NFATc1 plasmid (Open Biosystems) as the PCR template. PTBP1 3′-UTR was amplified from human genomic DNA with the primer pairs 5′-GAGAATTCCCTGGCGACAACTTCCATCATTC-3′ and 5′-GGTCTAGACACAATACTGAGCCTGGAATTGCTG-3′. The primer set for human CAMTA1 3′-UTR was 5′-GAGAATTCTGCGAGGGTAGTAATCATC-3′ and 5′-GGTCTAGACGAGGTTGGCAGTGAAAG-3′. To construct a mutated 3′-UTR reporter vector, four residues in the region that base-pairs with miRNA seeding sequences were mutated by using the QuikChange site-directed mutagenesis kit (Stratagene, La Jolla, CA). 293A was seeded onto 24-well plates and used for the 3′-UTR reporter assay. After the cells reached 80–90% confluence, the cells were transfected with 100 ng of 3′-UTR reporter vector, 700 ng of miR-124-expressing plasmid or mutated miR-124 plasmid, and 10 ng of phRL-TK using Lipofectamine 2000. The pENTR/CMV-EGFP without miRNA sequences was used as a control. Two days after transfection, the cells were harvested for the Dual-Luciferase activity assay.

Quantitative RT-PCR—To measure mRNA expression levels, total RNA was extracted with the miRNeasy minikit (Qiagen, Valencia, CA) and treated with an RNase-free DNase set (Qiagen). 1 μg of total RNA was reverse-transcribed using Moloney murine leukemia virus reverse transcriptase (Invitrogen) with oligo$(dT)_{18}$ plus random hexamer primers (Promega). qRT-PCR was performed with gene-specific primers and SYBR Green PCR Master Mix (Applied Biosystems, Foster City, CA) on an ABI 7300 real-time PCR system (Applied Biosystems). The expression level of each gene was normalized to the internal control, β-actin gene, and the expression level of each mRNA was calculated using the $2^{-\Delta\Delta}C_T$ method.

The mature miR-124 expression level was determined using our recently developed S-Poly(T) miRNA assay (27). The miR-124 expression level was normalized to the expression level of U6 (in human samples) or snoRNA-202 (in mouse samples) and calculated using the $2^{-\Delta\Delta}C_T$ method.

NFAT Dephosphorylation—Cells cultured on 6-well plates were co-transfected with 300 ng of pLVX/CMV-cMyc-NFATc2 and 1500 ng of plasmid encoding mature miR-124 (pENTR/CMV-EGFP-miR124a-2), miR-375 (pENTR/CMV-EGFP-miR-375), or EGFP without miRNA sequences (pENTR/CMV-EGFP). After a 2-day transfection period, cells were treated with 1 μM ionomycin for different times, and then the total proteins were extracted for Western blotting with c-Myc antibody to determine phosphorylated and dephosphorylated NFAT based on the change in their mobility. Using miR-375 as an unrelated control miRNA, the effect of miR-124 overexpression on the dephosphorylation of endogenous NFATc3 in 293T and HPASMC was determined by Western blotting with NFATc3 antibody.

NFAT Nuclear Translocation—First, we determined the effect of miR-124 on AcGFP-tagged NFATc1 nuclear translocation. U2-OS cells cultured on 24-well plates were co-transfected with 100 ng of pAcGFP-NFATc1 and 600 ng of plasmid encoding miR-124 (pUbc/miR-124a-2) or miR-375 (pUbc/miR-375) using Lipofectamine 2000. Another control group of pUbc/Control without miRNA sequence was also included. After 2 days of transfection, cells were treated with ionomycin (1 μM) and PMA (10 ng/ml) for 1 h and then fixed and stained with 4′,6′-diamidino-2-phenylindole dihydrochloride (DAPI; 300 nM; Molecular Probes, Inc. (Eugene, OR)). The AcGFP and DAPI images were taken from at least five different fields in each well and overlapped to determine whether AcGFP-NFATc1 localization was predominantly nuclear or cytoplasmic. Similar experiments were carried out on the same cell line by co-transfecting c-Myc-tagged NFATc2 plasmid (pLVX-

cMyc-NFATc2) and the plasmid expressing EGFP-tracked miR-124 (pENTR/CMV-EGFP-miR-124a-2), miR-375 (pENTR/CMV-EGFP-miR-375), or EGFP alone (pENTR/CMV-EGFP). After a 1-h stimulation with ionomycin/PMA, cellular localization of cMyc-NFATc2 was detected by immunostaining with an anti-tag primary antibody (c-Myc) followed by a Cy5-conjugated antibody.

Overexpression of miR-124 and IL-2 mRNA Expression Assay—One ml of lentivirus expressing primary human miR-124a-2 or its mutant miR-124a2m was used to transduct Jurkat T cells cultured in 100-mm dishes containing 8 μl/ml Polybrene. The infected Jurkat T cells were selected with puromycin (0.5 μg/ml) in the medium 2 days after infection. The same amount of selected Jurkat T cells were seeded onto 35-mm dishes and treated with ionomycin (0.5 μM) and PMA (10 ng/ml) for 6 h, and then the total RNAs were extracted, and the mRNA expression of IL-2 mRNA was detected by a qRT-PCR assay. The forward primer sequence is 5′-CCCAAGAAGGCCACAGAACT-3′. The reverse primer sequence is 5′-TGCTGATTAAGTCCCTGGGTCTTA-3′. For transient transfection, Jurkat T cells were transfected with 50 nM miR-124 mimic or mimic control (Ruibo Biotechnology, Guangzhou, China) by using Lipofectamine 2000. 6 h after transfection, cells were transferred into fresh medium and cultured for an additional 42 h. Then cells were either left untreated or treated with ionomycin/PMA for 6 h before total RNA extraction.

Western Blot—Cells were collected and dissolved in mRIPA mammalian protein extraction lysis buffer (50 mM Tris-HCl, pH 7.5, 150 mM NaCl, 1% Nonidet P-40, 0.25% sodium deoxycholate, and 1 mM EDTA) supplemented with protease inhibitor mixture (Roche Applied Science). The same amount of protein samples were fractionated by electrophoresis on SDS-PAGE and electroblotted to nitrocellulose membrane. After blocking with 5% fat-free milk in TTBS (20 mM Tris-HCl, pH 7.6, 150 mM NaCl, and 0.1% Tween 20), the blot was incubated with the corresponding primary antibodies followed by horseradish peroxidase-conjugated secondary antibodies (1:10,000 dilution). Then the membrane was developed with SuperSignal West Pico Chemi-luminescent Substrate (Thermo Scientific, Waltham, MA) and exposed to x-ray film. The primary antibodies used are as follows: mouse monoclonal anti-NFATc1 (1:1000 dilutions; Santa Cruz Biotechnology); rabbit anti-NFATc3 (1:500 dilutions; Santa Cruz Biotechnology); goat polyclonal anti-PTBP1 (1:1000; Abcam), mouse monoclonal anti-DsRed (1:3000; Clontech); rabbit polyclonal anti-CAMTA1 (1:500; Sigma); mouse monoclonal anti-c-Myc (1:3000; Sigma); mouse monoclonal anti-β-tubulin (1:5000; Sigma); rabbit polyclonal anti-PCNA (1:1000; Proteintech Group); mouse monoclonal anti-α-smooth muscle actin (α-SMA; 1:1000; Sigma).

Statistical Analyses—Each experiment was repeated at least three times. Data are presented as means ± S.D. Statistical analysis of the data was performed using a standard two-sample Student's *t* test. Statistical significance was determined using a two-tailed distribution assumption. *Asterisks* and *double asterisks* represent a significant difference between values of experimental pairs with $p < 0.05$ and $p < 0.01$, respectively.

RESULTS

High Throughput Screening of miRNAs in Regulating NFAT Signaling Pathway—We constructed an miRNA library overexpressing ~300 human primary miRNAs and performed the first round of screening in 96-well plates in duplicate using 293A cells and pGL4.30 NFAT luciferase reporter. The screening was done under unstimulated and PMA/ionomycin-stimulated conditions. Compared with the miRNA control vector, any miRNAs that changed the NFAT reporter activity with a >2-fold cut-off were considered as a hit. miRNAs that had error bars inside the cut-off were excluded. Using these criteria, 20 miRNAs were identified in an initial screening (Fig. 1*A*), which can be divided into six groups based on their effects on NFAT activity under unstimulated and/or stimulated conditions: 1) miR-124a-1, miR-124a-2, miR-124a-3, and miR-15b down-regulated NFAT signaling under both conditions; 2) miR-424 down-regulated under the unstimulated condition; 3) miR-367 down-regulated under the stimulated condition; 4) miR-524 up-regulated under the unstimulated condition; 5) miR-9–1, miR-29b-1, miR-339, miR-328, let-7f-2, miR-134, miR-150, miR-23b, let-7c, miR-330, miR-23a, and miR-125a up-regulated under the stimulated condition; and 6) miR-375 down-regulated under the unstimulated condition and up-regulated under the stimulated condition.

To confirm the results above, we performed a second round of screening in triplicate in 24-well plates. With the same criterion of a >2-fold cut-off value, 11 miRNAs (miR-424, miR-367, miR-29b-1, miR-339, miR-328, let-7f-2, miR-134, miR-150, miR-23b, let-7c, and miR-330) did not pass the second round of the screening (Fig. 1*B*). To further eliminate false positive hits, we used a backbone luciferase reporter plasmid containing a minimal promoter and luciferase gene but without the NFAT response element (pGL4.27) as an additional control. When each of the nine miRNAs that passed the second round of the screening was co-transfected with the pGL4.27 vector, only miR-375 significantly increased the luciferase activity under the stimulated condition (Fig. 1*C*). Therefore, miR-375 was excluded from the miRNA list linking to NFAT pathway and used as an unrelated control miRNA in this study. In summary, we identified eight miRNAs that regulate the NFAT pathway among ~300 miRNAs.

In silico analysis using miRbase showed that miR-124a-1, miR-124a-2, and miR-124a-3 are transcribed from different locations in the human genome but express the same mature sequence of miR-124. All three isoforms of miR-124 inhibited NFAT reporter activity (Fig. 1*B*). Because we were interested in the miRNAs with inhibitory effects on NFAT activity that might be developed as possible therapeutic agents in PAH where NFATs are activated in hypoxia-treated PASMC (13), we focused on miR-124 in subsequent studies.

miR-124 Represses NFAT Dephosphorylation—To further confirm the inhibitory effect of miR-124 on NFAT activity, we determined whether miR-124 could block the calcineurin-dependent dephosphorylation of NFAT in response to stimulation. NFATc2 was selected for the dephosphorylation assay because it has a very clear band in the Western blot, and also its molecular weight is relatively smaller than that of other NFAT

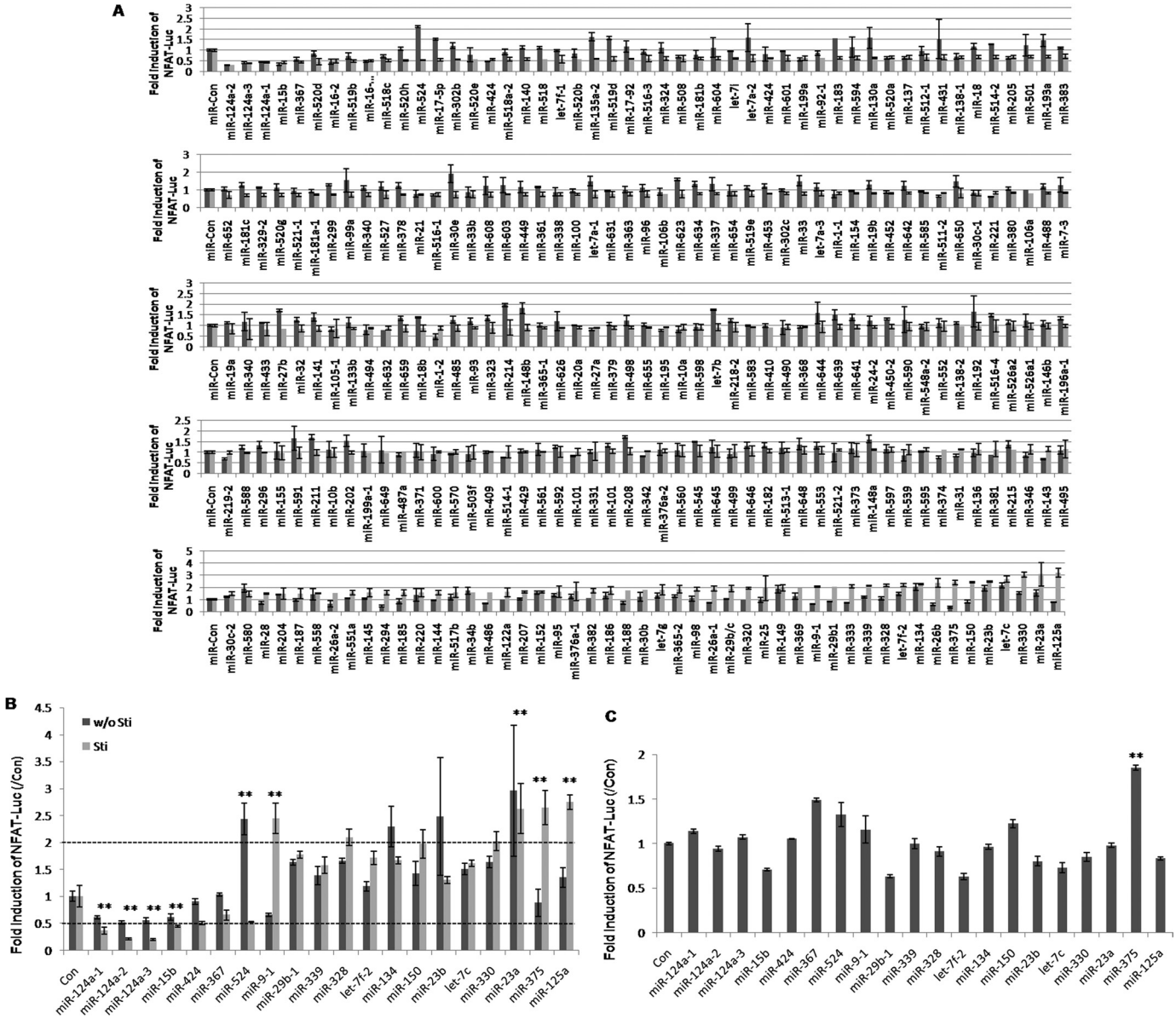

FIGURE 1. **Screening for miRNAs involved in the regulation of NFAT reporter activity in 293A cells.** *A*, 293A cells cultured on 96-well plates were transfected with a mixture of three plasmids: one expressing NFAT pathway firefly luciferase reporter (pGL4.30), another expressing *Renilla* luciferase (phRL-TK), and a third plasmid expressing EGFP-tracked pri-miRNA or miRNA control (miR-Con) of EGFP without any miRNA sequences. 32 h after transfection, cells were stimulated with PMA (10 ng/ml) and ionomycin (1 μM) for 12 h or left unstimulated for the same time and then lysed for Dual-Luciferase activity assays. firefly luciferase activities in lysates were normalized to those of *Renilla* luciferase for each transfection. The results were expressed as ratios of the relative luciferase activities over that in the miRNA control vector under unstimulated (*dark gray columns*) or stimulated (*dark gray columns*) conditions. *B*, from the initial screening, 20 miRNAs that changed the NFAT reporter activities by >2-fold were selected for further verification in 24-well plates under unstimulated and stimulated conditions. The results shown are means ± S.D. (*error bars*) ($n = 4$). **, $p < 0.01$ *versus* miRNA control. *C*, a backbone luciferase control vector, pGL3.27, was co-transfected with phRL-TK and a plasmid expressing miRNA or EGFP control (*Con*) to determine the background of reporter gene activity under the stimulated condition. The data are presented as means ± S.D. ($n = 4$). **, $p < 0.01$ *versus* control.

members. We co-transfected miR-124a-2, miR-375, or miRNA backbone EGFP control vectors with the c-Myc-tagged NFATc2 overexpression plasmid (pLVX/CMV-cMyc-NFATc2) into 293T cells and monitored the electrophoretic mobility of the c-Myc-NFATc2 after stimulation with ionomycin at different time points with anti-c-Myc antibody. The phosphorylated and dephosphorylated NFAT can be clearly distinguished based on its change in mobility on SDS-PAGE. NFATc2 proteins were dephosphorylated upon stimulation. However, overexpression of miR-124 significantly inhibited NFATc2 dephosphorylation (Fig. 2*A*). The dephosphorylation rate (defined as a ratio of dephosphorylation relative to phosphorylation) is shown in Fig. 2*A*. After 60 min of stimulation, the dephosphorylation rate of NFATc2 in the miR-124 overexpression group decreased more than 6-fold compared with that in the backbone EGFP control group (Fig. 2*A*). For miR-375, the dephosphorylated NFATc2 was higher than that of phosphorylated NFATc2 after 40 min of stimulation. Next, we measured the effect of miR-124 on the dephosphorylation of endogenous NFAT. As shown in Fig. 2*B*, overexpression of miR-124 inhibited the dephosphorylation of NFATc3 in ionomycin-stimulated 293T cells when compared with that in the overexpressed miR-375 control group. These

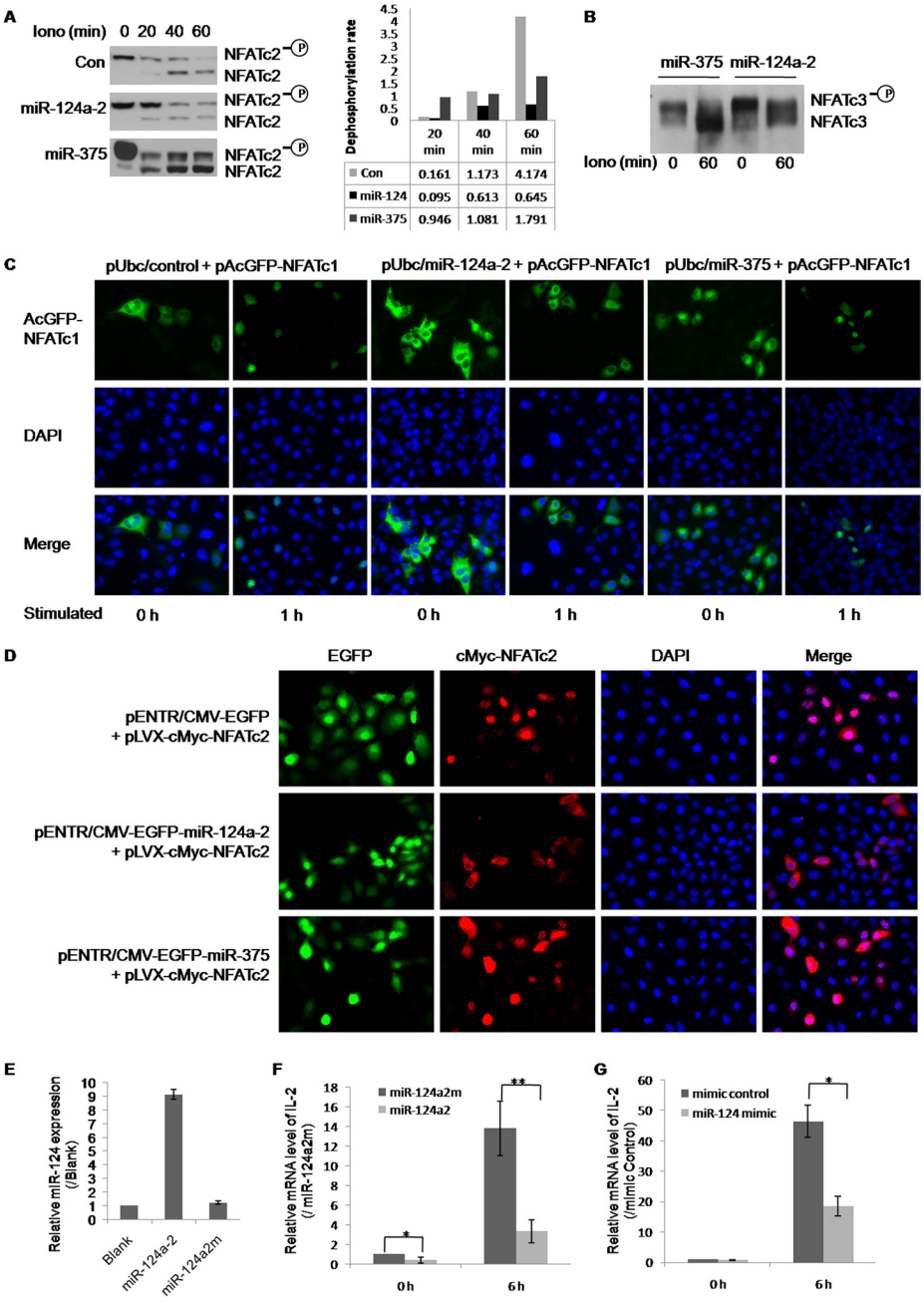

FIGURE 2. **miR-124 represses NFAT dephosphorylation, nuclear translocation, and its downstream target of IL-2.** *A*, 293T cells cultured on a 6-well plate were co-transfected with c-Myc-tagged NFATc2 overexpressing plasmid (pLVX/CMV-cMyc-NFATc2) and a plasmid encoding miR-124a-2 (pENTR/CMV-EGFP-miR-124a-2), miR-375 (pENTR/CMV-EGFP-miR-375), or pENTR/CMV-EGFP control vector (*Con*). Two days after transfection, cells were treated with 1 μM ionomycin for 0, 20, 40, or 60 min, and the total proteins were then extracted for Western blot with anti-c-Myc antibody. The dephosphorylation rate of NFATc2, defined as a ratio of the intensity in dephosphorylated NFATc2 (*bottom band*) over that in the phosphorylated form (*top band*), was calculated according to the Western blot data. *B*, 293T cells were transfected with the plasmid encoding miR-124a-2 (pENTR/CMV-EGFP-miR-124a-2) or miR-375 (pENTR/CMV-EGFP-miR-375). Two days after transfection, cells were left or treated with 1 μM ionomycin (*Iono*) for 60 min, and the total proteins were then extracted for Western blot with NFATc3 antibody. The phosphorylated and dephosphorylated NFATc3 are indicated. *C*, U2-OS cells on 6-well plates were co-transfected with pAcGFP-NFATc1 and plasmid pUbc/miR-124a-2, pUbc/miR-375, or pUbc/Control. Two days after transfection, cells were stimulated with ionomycin (1 μM)/PMA (10 ng/ml) for 1 h or left unstimulated for the same time and then fixed and stained with DAPI. The AcGFP and DAPI images were taken from at least five different fields in each well and overlapped (*Merge*) to determine AcGFP-NFATc1 nuclear localization. *D*, U2-OS cells were co-transfected with pLVX-cMyc-NFATc2 and the plasmid expressing mature miR-124 (pENTR/CMV-EGFP-miR-124a-2), miR-375 (pENTR/CMV-EGFP-miR-375), or EGFP alone vector (pENTR/CMV-EGFP). Two days after transfection, cells were stimulated with ionomycin (1 μM)/PMA (10 ng/ml) for 1 h and then fixed and stained with anti-c-Myc primary antibody followed by a Cy5-conjugated secondary antibody. The localization of cMyc-NFATc2 (*red color*) and co-transfected miRNA with EGFP maker were determined under an inverted fluorescence microscope. DAPI nuclear staining was merged with the *red color* to determine the cMyc-NFATc2 cellular localization. *E*, Jurkat T cells were infected with lentivirus encoding wild-type miR-124a-2 or its mutant (miR-124a2m) and selected with puromycin for a week. The expression level of miR-124 was detected by qRT-PCR. The values are shown relative to the value obtained from blank control without viral infection. *F*, the mRNA expression level of IL-2 was measured by qRT-PCR in the stable selected Jurkat T cells overexpressing miR-124 or its mutant before and after 6-h stimulation with ionomycin (0.5 μM) and PMA (10 ng/ml). β-Actin was used as a reference. Data shown are relative to miR-124a2m before stimulation. $n = 3$; *, $p < 0.05$; **, $p < 0.01$. *G*, using Lipofectamine 2000 transfection reagent, 50 nM miR-124 mimic or mimic control was transfected into Jurkat T cells. Two days after transfection, cells were stimulated with ionomycin/PMA for 6 h or left unstimulated for the same time. Using β-actin as reference, the expression level of IL-2 were quantified by qRT-PCR. The value was shown as -fold change relative to mimic control before stimulation ($n = 3$; *, $p < 0.05$). *Error bars*, S.D.

results further support our contention that miR-124 has a role in negative regulation of NFAT activity.

miR-124 Represses Nuclear Translocation of NFAT—Because the translocation of dephosphorylated NFAT from the cytoplasm to the nucleus is essential for the subsequent activation of its target genes, we examined the effect of miR-124 overexpression on NFAT nuclear translocation. U2-OS cells were chosen for this experiment because of their good morphology and adherence after fixation (28). We co-transfected U2-OS cells with CMV promoter-driven pAcGFP-NFATc1 vector and Ubc promoter-driven plasmid encoding mature miR-124 (pUbc/miR-124a-2), miR-375 (pUbc/miR-375), or pUbc/Control vector, and the distribution of AcGFP-NFATc1 fusion protein was monitored directly using an inverted fluorescent microscope. The reason we used the Ubc promoter to drive miRNA expression was to avoid promoter competition and thus significantly increase the fluorescent signal of AcGFP-NFATc1 (data not shown). In the resting cells, almost all AcGFP-NFATc1 fusion protein remained in the cytoplasm. Stimulation with ionomycin/PMA for 1 h led to a dramatic nuclear translocation of AcGFP-NFATc1 (Fig. 2*C*). However, miR-124 overexpression caused nearly complete retention of AcGFP-NFATc1 in the cytoplasm despite stimulation with ionomycin/PMA when compared with that in the miR-375 overexpression group or the backbone control (Fig. 2*C*). To further investigate if miR-124 affects the translocation of other NFATs, U2-OS cells were co-transfected with c-Myc-tagged NFATc2 vector and EGFP-tracked miR-124a-2, miR-375, or EGFP only vectors. Similar results were observed, and miR-124 retained most of the cMyc-NFATc2 in the cytoplasm despite stimulation with ionomycin/PMA (Fig. 2*D*). Therefore, in addition to repression of NFAT dephosphorylation, miR-124 also prevents NFAT nuclear translocation and thus eventually inhibits NFAT activity.

miR-124 Inhibits IL-2 Transcription—To examine the effect of miR-124 on the downstream target of NFAT transcription factor, we stimulated cells overexpressing miR-124 or its mutant with ionomycin/PMA for 6 h and then analyzed the expression of endogenous IL-2 by qRT-PCR. As shown in Fig. 2*E*, the mature wild-type miR-124 was increased nearly 10-fold compared with the blank control or mutated miR-124. The expression of IL-2 mRNA before and after stimulation was significantly lower in miR-124-overexpressing Jurkat T cells when compared with its mutation control (Fig. 2*F*). In addition, we evaluated the effect of chemically synthesized miR-124 mimics or mimic controls on IL-2 expression in Jurkat T cells under both unstimulated and stimulated conditions. Similar to what we observed in stable expression cells, the IL-2 mRNA expression level was significantly decreased in the miR-124 mimic-treated group compared with the mimic control under the stimulated condition (Fig. 2*G*). These results are consistent with the previous NFAT-Luc reporter assay as well as the NFAT dephosphorylation and translocation assays, further demonstrating the inhibitory effect of miR-124 on NFAT transactivation.

Validation of NFATc1 as a Direct Target of miR-124—The data above suggest that miR-124 could be suppressing the signaling molecules involved in NFAT activation. To understand the mechanism by which miR-124 inhibits the NFAT pathway, we applied the TargetScan program to predict potential target genes of miR-124. We only chose those molecules relevant to NFAT activation. We also selected several known genes targeted by miR-124. The combination of these analyses resulted in 14 potential targets of miR-124 that may be involved in the NFAT pathway (Table 1). Among them, one of the NFAT members, NFATc1 is the predicted target of miR-124. There are two putative binding sites (BS1 and BS2) downstream of the stop codon at 369–376 and 1357–1363 in the mouse NFATc1 3′-UTR, which are well conserved among human, mouse, rat, and other species (TargetScan version 4.2). The two binding sites have perfect complementarity to the seed region (positions 2–8) (Fig. 3*A*). The 3′-UTR luciferase assays revealed that all of the miR-124 isoforms (pENTR/CMV-EGFP-miR-124a-1, pENTR/CMV-EGFP-miR-124a-2, and pENTR/CMV-EGFP-miR-124a-3) significantly suppressed NFATc1 3′-UTR reporter luciferase activity compared with EGFP control vector (*Con*) (Fig. 3*B*). Although miR-15b down-regulates NFAT pathway luciferase reporter activity, it did not affect NFATc1 3′-UTR reporter luciferase activity at all. The seeding region is believed to be essential in target recognition. We therefore constructed a mutant of miR-124 expression vector (pENTR/CMV-EGFP-miR-124a2m) by introducing a 5-nucleotide substitution mutation in the seeding sequence of miR-124a-2. Although wild-type miR-124a-2 suppressed ~67% of luciferase activity, the mutated miR-124 (miR-124a2m) had no effect on the reporter activity (Fig. 3*B*).

Next, we sought to identify which site is necessary for the binding of miR-124 to the 3′-UTR of NFATc1 by introducing a 4-nucleotide substitution mutation at each binding site (BS1-mut and BS2-mut). Compared with the wild type 3′-UTR, the mutations at the BS1 or BS2 binding site caused a decrease in inhibition from an average of 60% to 34 or 16%, respectively (Fig. 3*C*), indicating that both sites may be involved in binding, although the second site appears to be more important.

To further confirm the binding of miR-124 to NFATc1 3′-UTR, we co-transfected miR-124a-2 overexpression vector and AcGFP-NFATc1 expression vector with or without NFATc1 3′-UTR (Fig. 3*D*) into 293A cells. For the normalization of transfection efficiency, the same amount of pDsRed2-C1 vector was included in each transfection. As shown in Fig. 3*E*, overexpression of miR-124 significantly reduced the AcGFP-NFATc1 fusion protein level with 3′-UTR but not that without

TABLE 1
The siRNA sequences against the predicted targets of miR-124

miR-124 target	siRNA sequence (5′–3′)	Reference/Source
Ctdsp1	GCTCATCCTGGACAATTCA	Ref. 54
Ctdsp2	GCTGAACCTGATCCCAATC	Ref. 54
PTBP1	CAATGACAAGAGCCGTGACT	Ref. 55
Lamc1	CCTTACCATCTGGCTGCTTC	Ref. 56
CEBPA	CGACGAGTTCCTGGCCGAC	Ref. 57
ITGB1	GGATATTACTCAGATCCAA	Ref. 58
Stx2	GCTATTGAACAAAGTTTC	Our design
TOM1LI1	AATGCTATCCTTGGATATGA	Ref. 59
SypI	GCCTACACAGTCCATCAAAT	Our design
Arfip1	CGCAATGATGTTTCTGTCAA	Our design
MAPK14	CTCTCCAAATATTATTCAA	Ref. 58
CHP	AGAGCAAAGATGTGAATGGA	Ref. 60
LIFAT	GACAGTGGCTGTTAACAGTT	Our design
CAMTA1	GCCATCCTTATCCAGAGCAA	Our design
NFATc1	GGTCATTTTCGTGGAGAAAG	Our design

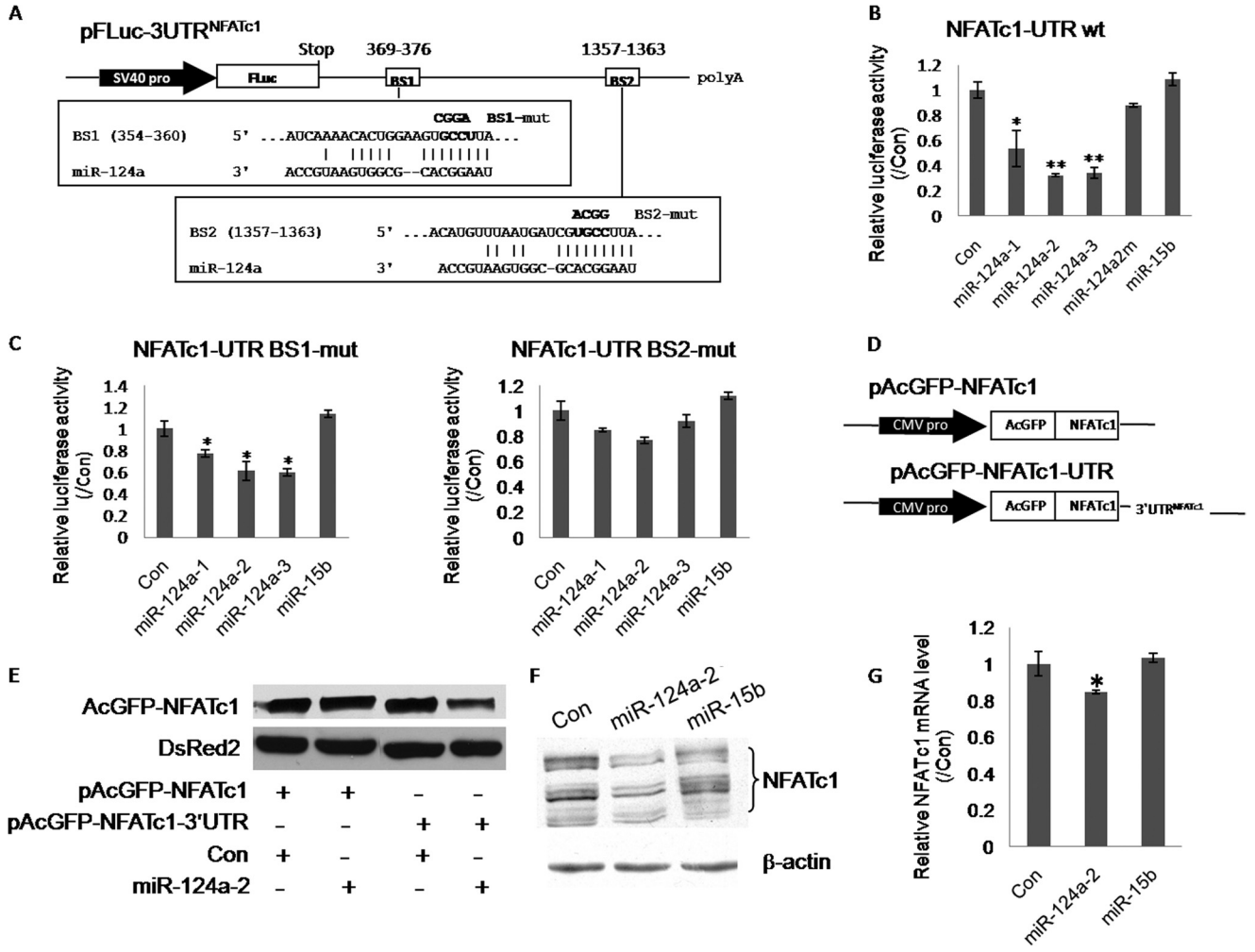

FIGURE 3. **Verification of NFATc1 as a direct target of miR-124.** *A*, a diagram of mouse NFATc1 3′-UTR luciferase reporter construct (pFLuc-3′UTR^{NFATc1}) with predicted miR-124 binding sites (BS1 and BS2). The mutated binding sites in pFLuc-3UTR^{NFATc1} vector are indicated in *boldface type*. *B*, 293A cells were co-transfected with pFLuc-3′UTR^{NFATc1}, phRL-TK, and the plasmid encoding mature miR-124 (pENTR/CMV-EGFP-124a-1, pENTR/CMV-EGFP-124a-2, pENTR/CMV-EGFP-124a-3), mutated miR-124a2m (pENTR/CMV-EGFP-124a-2m), miR-15b, or control EGFP vector (*Con*). After a 2-day transfection, cells were lysed for the Dual-Luciferase assay. Firefly luciferase activities were normalized with *Renilla* luciferase activities. The results were expressed as a ratio of the relative luciferase activities over that in the control vector. The graph shows the means ± S.D. (*error bars*) ($n = 3$; *, $p < 0.05$; **, $p < 0.01$ *versus* control). *C*, 293A cells were co-transfected with pFLuc-3UTR^{NFATc1} vector mutated at each predicted binding site (NFATc1-UTR BS1-mut or NFATc1-UTR BS2-mut), phRL-TK, and the plasmid encoding miR-124a-1, -2, -3, miR-15b, or EGFP control vector. Relative luciferase activities were measured after 2 days transfection. The binding site was determined according to normalized luciferase activities relative to that of control. *D*, schematic diagrams of the constructs of pAcGFP-NFATc1 without NFATc1 3′-UTR and pAcGFP-NFATc1–3′UTR with NFATc1 3′-UTR. *E*, pAcGFP-NFATc1 or pAcGFP-NFATc1–3′UTR were transfected into 293A cells together with either pENTR-EGFP-miR-124a-2 vector or pENTR-EGFP control vector. The pDsRed2-c1 vector was also included in each transfection for the normalization of transfection efficiency. Two days after transfection, the expression levels of AcGFP-NFATc1 fusion proteins and DsRed2 were measured by Western blots. DsRed2 was used to normalize the transfection efficiency. *F* and *G*, 293A cells were infected with lentivirus encoding miR-124a-2, miR-15b, or EGFP control. The expression levels of endogenous NFATc1 protein and mRNA were determined by Western blot and qRT-PCR, respectively, using β-actin as a reference. The values shown in *G* are relative to those obtained with EGFP control ($n = 3$; *, $p < 0.05$ *versus* control).

3′-UTR, further demonstrating an essential role of the NFATc1 3′-UTR in the suppressive effect of miR-124 on NFATc1 expression.

To examine whether miR-124 negatively regulates endogenous NFATc1 protein level, we performed Western blot analysis on 293A cells transfected with a lentivirus overexpressing miR-124, miR-15b, or control EGFP. We observed a significant decrease of NFATc1 protein in the miR-124-overexpressing cells compared with the cells transfected with miR-15b or EGFP control lentivirus (Fig. 3*F*). Regulation of gene expression by miRNA can occur through inhibition of protein translation and/or by decreasing mRNA amounts. As revealed by qRT-PCR (Fig. 3*G*), the mRNA level of NFATc1 in miR-124-overexpressing cells was only decreased by about 15% compared with control cells, indicating that miR-124 regulates NFATc1 mRNA stability to a limited extent.

Elucidation of Multiple Targets of miR-124; CAMTA1 and PTBP1 and Their Roles in NFAT Pathway—Although our data have verified NFATc1 as a direct target of miR-124, the suppressive effect of miR-124 on the upstream events, NFAT dephosphorylation and translocation, suggests that miR-124 may target other genes that are critical to NFAT dephosphorylation or translocation.

To identify other potential targets that may positively regulate the NFAT pathway, we constructed a series of shRNA vectors, namely pENTR/shRNA, against the putative target genes

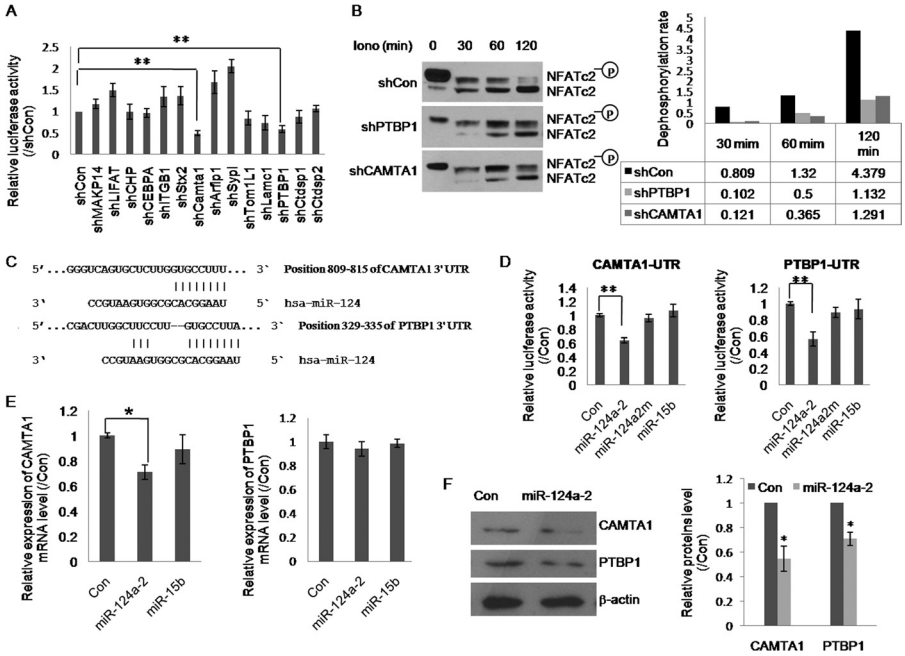

FIGURE 4. **Identification of miR-124 targets associated with NFAT activation.** *A*, the effect of silencing predicted miR-124 targets on NFAT reporter activity under the stimulated condition. 293A cells were co-transfected with pGL4.30, phRL-TK, and each predicted targeting gene silencing vector. Two days after transfection, cells were stimulated with PMA (10 ng/ml) and ionomycin (1 μM) for 12 h and then lysed for the Dual-Luciferase activity assay. The relative luciferase activity (firefly luciferase/*Renilla* luciferase) was normalized to that of the shCon group. Three independent experiments were repeated and conducted in triplicates. Data are expressed as mean $\pm$ S.D. **, $p < 0.01$ *versus* shCon. *B*, 293T cells were co-transfected with pLVX/CMV-cMyc-NFATc2 and the plasmid expressing shPTBP1, shCAMTA1, or shCon. Two days after transfection, cells were stimulated with ionomycin for different times (0, 30, 60, and 120 min), and the dephosphorylation rates of NFATc2 in the cell lysates were examined and calculated by Western blots using anti-c-Myc antibody. *C*, schematic diagrams of mature miR-124 sequence and its potential binding site in the 3′-UTR of human CAMTA1 and BTBP1. *D*, firefly luciferase reporter vector containing the CAMTA1 or BTBP1 3′-UTR (pFLuc-3′UTR^{CAMTA1}, pFLuc-3′UTR^{BTBP1}) was co-transfected into 293A cells with phRL-TK and the plasmid expressing miR-124a-2, mutated miR-124a2m, miR-15b, or EGFP control (*Con*). Two days after transfection, the cells were collected for the Dual-Luciferase assay. The values shown are normalized luciferase activities relative to those in EGFP control ($n = 3$; **, $p < 0.01$). *E*, using β-actin as an internal reference, the expression levels of CAMTA1 and PTBP1 in 293A cells overexpressing miR-124a-2, miR-15b, or EGFP control were determined by qRT-PCR. The values shown are relative to those obtained with the EGFP control group ($n = 3$; *, $p < 0.05$ *versus* control). *F*, Western blot analysis showed that overexpression of miR-124 resulted in the reduction of endogenous CAMTA1 and PTBP1 proteins in 293A cells compared with the EGFP control group. β-Actin was used as a loading control. Western blot data were quantified to better view the difference between different treatment groups.

(as listed in Table 1) and performed an NFAT reporter assay under the stimulated condition. As shown in Fig. 4*A*, silencing of CAMTA1 and PTBP1 caused the largest inhibition of the NFAT reporter activity (~51 and 42%, $p < 0.01$) compared with the control shRNA group. Knockdown of CAMTA1 or PTBP1 also decreased the dephosphorylation rate of c-Myc-tagged NFATc2 compared with shCon (Fig. 4*B*). These results suggest that CAMTA1 and PTBP1 may be involved in the positive regulation of the NFAT pathway.

TargetScan analysis showed that there was one putative binding site of miR-124 in the 3′-UTR of CAMTA1 and PTBP1 (809–815 and 329–335, respectively) (Fig. 4*C*). To experimentally verify this prediction, we cloned 3′-UTR regions of human CAMTA1 and PTBP1 into the pGL3-control luciferase reporter vector. When the miR-124a-2 expression plasmid was co-transfected into the cells with the CAMTA1 or PTBP1 3′-UTR luciferase reporter construct, the reporter luciferase activities were repressed by about 36 and 44%, respectively (Fig. 4*D*). However, the inhibition was almost abolished when cells were transfected with the mutated miR-124 (miR-124a2m) or miR-15b overexpression vectors.

We next determined the endogenous mRNA levels of CAMTA1 and PTBP1 in the miR-124-overexpressing 293A cells. Compared with the EGFP control vector (*Con*) or miR-15b, miR-124 decreased the CAMTA1 mRNA level by 32% but had no effects on PTBP1 mRNA expression (Fig. 4*E*). However, the protein levels of both BTBP1 and CAMTA1 in the miR-124-overexpressing 293A cells were significantly lower than those in control cells (Fig. 4*F*). These data demonstrate that CAMTA1 and PTBP1 are direct targets of miR-124.

miR-124 Was Down-regulated in both Hypoxia-treated HPASMC and Chronic Hypoxia-induced PAH Mouse Lungs—NFATs are essential for the development of PAH in both human patients and chronic hypoxia-induced PAH animal models (11, 12). It has been reported that NFATs are activated by hypoxia treatment in PASMC (10, 13). In these studies, we also observed that NFATc3, one of the major isoforms of NFATs in HPASMC, was activated by hypoxia treatment according to an NFAT dephosphorylation assay (Fig. 5*A*). To determine if miR-124-mediated NFAT suppression occurs in pulmonary artery smooth muscle cells, several key experiments were performed in HPASMC. First, we examined the effect of miR-124 on NFAT reporter activity. As shown in Fig. 5*B*, overexpression of miR-124a-2 significantly inhibited NFAT reporter activity in stimulated HPASMC when compared with EGFP control or miR-375. Then we examined the effect of hypoxia treatment on endogenous NFATc3 in HPASMC stably expressing miR-124 or miR-375. Similar to the observation in 293A cells (Fig. 2*B*), overexpression of miR-124 but not miR-375 inhibited the dephosphorylation of endogenous NFATc3 in

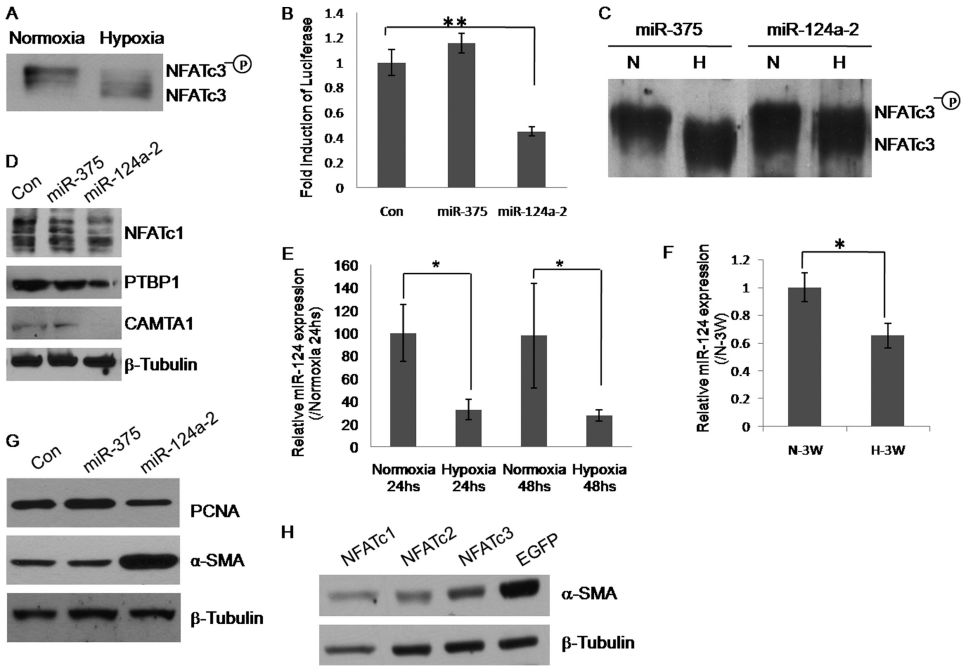

FIGURE 5. **Reduced expression of miR-124 in hypoxia HPASMC and chronic hypoxia-induced PAH mice and its antiproliferative and prodifferentiation effects.** *A*, the same number of HPASMC were cultured under normoxic or hypoxic (3% O_2) conditions for 24 h, and the total proteins were then extracted for Western blot with NFATc3 antibody. *B*, HPASMC cultured on 24-well plates were co-transfected with pGL4.30, phRL-TK, and the plasmid encoding miR-124a-2 (pENTR/CMV-EGFP-miR-124a-2), miR-375 (pENTR/CMV-EGFP-miR-375), or EGFP control (*Con*). Two days after transfection, cells were stimulated with PMA (10 ng/ml) and ionomycin (1 μM) for 12 h and then lysed for the Dual-Luciferase activity assay. Firefly luciferase activities were normalized with *Renilla* luciferase activity. The values shown are relative to those obtained with control ($n = 3$; **, $p < 0.01$). *C*, HPASMC infected with lentivirus encoding miR-124 or miR-375 were cultured at normoxia (*N*) or hypoxia (*H*) for 24 h. The total proteins were then extracted for Western blot with anti-NFATc3 antibody to determine the dephosphorylation of NFATc3. *D*, HPASMC infected with lentivirus encoding mature miR-124, miR-375, or EGFP control were lysed, and the cell lysates were used to determine the protein levels of three targets (NFATc1, PTBP1, and CAMTA1). The amount of β-tubulin was used as a loading control. *E*, the same amount of HPASMC were cultured at normoxia or hypoxia for 24 or 48 h, and then the expression levels of miR-124 were measured by qRT-PCR using U6 as a normalization control. The values shown are relative to those obtained under each normoxia condition ($n = 4$; *, $p < 0.05$). *F*, mice were exposed to normoxia (ambient air; *N-3W*) or hypoxia (10% O_2; *H-3W*) for 3 weeks, and then the expression level of miR-124 in mouse lungs was examined by qRT-PCR using snoRNA-202 as a reference. Data are presented as mean ± S.D. and compared with those exposed to normoxia. *, $p < 0.05$; $n = 3$ for each group. *G*, the same amount of HPASMC transduced with lentiviral vectors encoding miR-124, miR-375, or EGFP were lysed for Western blots with antibodies against PCNA, α-SMA, or β-tubulin (as a loading control). *H*, effect of NFATc1, -c2, or -c3 overexpression on HPASMC differentiated phenotype. HPASMC transduced with lentiviral vectors overexpressing NFATc1, -c2, or -c3 or EGFP control were lysed, and α-SMA was determined by Western blot analysis. The amount of β-tubulin was selected as a loading control. *Error bars*, S.D.

hypoxia-treated HPASMC. Furthermore, we found that all three targeting proteins (NFATc1, PTBP1, and CAMTA1) were decreased in miR-124-overexpressing HPASMC compared with EGFP control or the miR-375 group (Fig. 5*D*). Taken together, these results suggest that miR-124 plays similar roles in HPASMC as observed in 293A cells.

To determine if miR-124 expression correlates with hypoxia-induced NFAT activation, we examined the expression level of endogenous miR-124 by qRT-PCR in hypoxia-treated HPASMC and chronic hypoxia-exposed mouse lungs. As shown in Fig. 5*E*, the expression levels of miR-124 in 24- and 48-h hypoxia-treated HPASMC decreased by 67 and 72%, respectively. Similar results were obtained in the rat A7r5 smooth muscle cell line (data not shown). Because chronic hypoxia is a well established stimulus for induction of PAH in experimental rodent models, we measured the expression level of miR-124 in chronic hypoxia-exposed mouse lungs as described in our previous study (22). As shown in Fig. 5*F*, the expression level of miR-124 was decreased ~35% in mouse lungs after 3 weeks of hypoxia treatment compared with that in normoxia control. These data demonstrate for the first time that miR-124 is down-regulated by hypoxia not only in cells but also *in vivo* in remodeled lung tissues, further implying that down-regulation of miR-124 by hypoxia may contribute to NFAT activation during PAH development.

Forced Expression of miR-124 Induces Potent Antiproliferative and Prodifferentiation Effects in HPASMC—To evaluate the biological functions of miR-124 in HPASMC, we infected HPASMC with lentivirus overexpressing miR-124, miR-375, or EGFP control and assessed the changes in the cell proliferation marker (PCNA) by Western blotting. Compared with EGFP control or miR-375, overexpression of miR-124a-2 significantly reduced the expression of the proliferative marker PCNA (Fig. 5*G*), demonstrating that miR-124 may play a role in modulating HPASMC proliferation. We further analyzed the effects of miR-124a-2 overexpression on cell differentiation by measuring the smooth muscle cell-specific marker, α-SMA. We found that α-SMA was dramatically up-regulated in the miR-124a-2-overexpressing cells (Fig. 5*G*). To determine whether miR-124-induced up-regulation of α-SMA is mediated through its inhibitory effects on the NFAT pathway, we overexpressed NFATc1, NFATc2, and NFATc3, respectively, and examined their effects on smooth muscle cell-specific marker by Western blot analysis. Our results showed that overexpression of each NFAT member led to a significant decrease of α-SMA (Fig. 5*H*), indicating that miR-124-induced prodifferentiation effects on

HPASMC might be mediated through its inhibition of the NFAT pathway.

DISCUSSION

In this study, we screened potential miRNAs involved in NFAT regulation and found that miR-124 had the highest inhibitory effect on NFAT transactivation via targeting multiple genes, NFATc1, CAMTA1, and PTBP1. The inhibitory effect of miR-124 on the NFAT pathway was further confirmed by its roles in NFAT dephosphorylation, nuclear translocation, and the expression of NFAT downstream target (IL-2). This is the first report of decreased expression of miR-124 induced by hypoxia in both HPASMC and chronic hypoxia-induced PAH mouse lungs, which is consistent with the finding that hypoxia induces NFAT activation. Functionally, we found that miR-124 has potent antiproliferative and prodifferentiation effects in human pulmonary artery smooth muscle cells, probably through its inhibition of the NFAT pathway.

We utilized a simple cell-based model in which we combined an miRNA expression library with the NFAT-responsive luciferase reporter for high throughput screening of potential miRNAs involved in the regulation of NFAT signaling pathway. This strategy is a robust one for quick screening of mRNA/miRNAs involved in different signaling pathways. Previously, Willingham *et al.* (28) developed this strategy with NFAT luciferase reporter vector and an arrayed shRNA library against 512 conserved non-coding RNAs for a functional screening of non-coding RNAs involved in NFAT regulation and identified an important non-coding RNA repressor of NFAT. miRNAs are now known to play a variety of important regulatory roles in both plants and animals. To date, 1872 human precursor miRNAs have been deposited in the Sanger miRNA database (29). Bioinformatic prediction suggests that they regulate up to ~60% of human genes (30). However, the functions of only a small fraction of miRNAs have been determined (31). A few miRNAs linked to NFAT regulation have been identified: miR-184 targets NFATc2 (32); miR-133a targets NFATc4 (23); miR-199b targets the nuclear kinase Dyrk1a (33), which limits calcineurin/NFAT signal transduction by phosphorylating NFAT; and miR-1 negatively regulates the NFAT signal pathway by targeting calmodulin, which is a crucial mediator of calcium signaling (34). In addition, it has been reported that miR-23a is controlled by NFAT at the transcriptional level (24). In this study, of 300 miRNAs, we identified miR-124 and miR-15b as suppressors of the NFAT signal pathway and miR-125a, miR-23a, and miR-9-1 as stimulators under a stimulated condition. Another interesting miRNA that we identified is miR-524, which regulates NFAT positively under an unstimulated condition but negatively under a stimulated condition. Among these identified miRNAs, it has been reported that miR-23a is up-regulated by the NAFTc3 pathway (24). We focused on miR-124 and elucidated how miR-124 suppresses NFAT activation in response to stimuli because we wish to develop an miRNA-based NFAT suppressor.

Although miR-124 has been shown to be involved in regulation of multiple target genes (35–38), it is notable that our data provide the first evidence for a regulatory role of miR-124 in the NFAT pathway. *In silico* analyses using miRbase show that miR-124 has three precursor hairpin sequences in the human genome: miR-124a-1, miR-124a-2, and miR-124a-3, located on chromosome 20, 20, and 8, respectively. During the initial screening with the miRNA library, we observed that all three primary miR-124 expression vectors could reduce NFAT-responsive luciferase activities to a similar extent. The inhibitory effect of miR-124 on the NFAT pathway was further confirmed during the second round of verification. The inhibition of NFAT signaling could be by inhibiting calcium mobilization, preventing calmodulin activation, inhibiting calcineurin, preventing calcineurin from docking onto NFAT, activating NFAT kinases, interfering with the NFAT nuclear import process, or even direct targeting to the NFAT gene itself (39). We have identified that miR-124 suppresses NFAT activity by regulating its NFAT phosphorylation and subsequent nuclear translocation, two major steps involved during calcium-induced NFAT signaling. Furthermore, we have shown that overexpression of miR-124 can significantly inhibit the activation of the NFAT pathway, opening the door for the development of a new miRNA-based immunosuppressant.

To understand the molecular mechanism of miR-124-mediated NFAT inhibition, we predicted miR-124 target genes with bioinformatics software and selected a group of genes potentially associated with the NFAT pathway for further analysis. Among them, one of the isoforms, NFATc1, was identified as a new target of miR-124. According to our finding that miR-124 can control phosphorylation and nuclear translocation of other NFATs, NFATc1 definitely is not the only target of miR-124. Therefore, as in the initial screening step, we silenced 13 predicted targets by the RNAi technique and then performed an NFAT reporter assay. Because miR-124 negatively regulates NFAT activation, silencing its target should inhibit NFAT activation. Of 13 predicted genes, knockdown of CAMTA1 and PTBP1 showed the most significant inhibition of NFAT reporter activity. The dephosphorylation rate assay also provided consistent evidence that both CAMTA1 and PTBP1 are involved the control of NFAT activation. We further confirmed that these two genes are direct targets of miR-124 using the 3′-UTR luciferase assay and Western blot analysis. Thus, we propose that miR-124 suppresses NFAT activity by targeting multiple genes, including NFATc1, CAMTA1, and PTBP1.

PTBP1 (polypyrimidine tract-binding protein 1) is an RNA-binding protein that is a specific mRNA splicing repressor in the mammalian nervous system. It has been previously reported that PTBP1 is one of the direct targets of miR-124 (40, 41). CAMTA1 (calmodulin-binding transcription activator 1) is a putative transcription factor (42). CAMTA family members respond to Ca^{2+} signaling by binding to calmodulin (43). CAMTA1 acts as both an integrator and effector of Ca^{2+} signaling and may mediate Ca^{2+}-dependent processes in neuronal differentiation (42). In our studies, we found that both PTBP1 and CAMTA1 were involved in the regulation of the NFAT signaling pathway, providing the linkage between miR-124 and the NFAT pathway. Further investigations are needed to define how PTBP1 and CAMTA1 regulate the NFAT pathway.

miR-124 was initially described as a brain-specific miRNA that is associated with various nervous system diseases, such as Alzheimer disease and medulloblastoma (35, 40, 44–46). How-

ever, several reports have shown that miR-124 is also expressed in non-neuron tissues/cells, such as pancreas (47), breast (11), bone marrow-derived mesenchymal stem cells (48), and lung (49), and has functions in these tissues. Pulmonary artery smooth muscle cells in the adult are highly specialized cells that regulate vessel tone through the expression of a unique repertoire of SMC-specific genes, such as α-SMA, SM22α, smooth muscle myosin heavy chain (SM-MHC), and calponin (50). Unlike terminally differentiated muscle cells, PASMC are remarkably plastic and can modulate their phenotype from a contractile to proliferative, synthetic type in response to vascular injury (9, 50). Because hypoxia-induced proliferation of PASMC has been linked to NFAT activation (10), we measured the expression of miR-124 in both primary culture of HPASMC and whole lungs before and after hypoxia treatments. We found that the expression of miR-124 was significantly decreased by hypoxia both in cells in culture and in whole lungs *in vivo*. More importantly, we found that ectopic expression of miR-124 decreased HPASMC proliferation. This is consistent with previously published data indicating that miR-124 is less expressed in proliferative cells and can reduce cell proliferation (45). For instance, overexpression of miR-124 resulted in reduced proliferation of neural progenitors (51) and glioblastoma multiforme cells (52). Our results reveal a potential mechanism by which miR-124 expression may be suppressed by hypoxia, which in turn results in increased cell proliferation via the NFAT pathway.

Previous studies have demonstrated that cell differentiation is enhanced by ectopic overexpression of miR-124 in mouse ES cells (53), neuroblastoma cells, and embryonic carcinoma cells (40). In concordance with these results, we found that overexpression of miR-124 promoted a remarkable increase in expression of the contractile phenotype marker, α-SMA, in HPASMC. Then we determined if the prodifferentiation effect of miR-124 is mediated by the NFAT signaling pathway. We hypothesized that if miR-124-induced cell differentiation is mediated by NFAT, overexpression of NFAT should decrease the expression of α-SMA. Our data clearly show that ectopic overexpression of three different NFAT isoforms significantly down-regulated the protein level of α-SMA. Based on these results, we propose that miR-124 may play a role in promoting a contractile, differentiated phenotype in PASMC by inhibiting the NFAT pathway. However, this conclusion conflicts with other reports in which NFAT is considered to be a positive regulator of α-SMA promoter activity (12). We performed similar experiments by co-transfecting an α-SMA promoter-driven luciferase reporter and NFATc1, NFATc2, or NFATc3 overexpression vector. Similar to the previous report, overexpression of NFAT did increase the α-SMA promoter activity by ~30%. Apparently, the suppressive effect of NFAT on α-SMA might come from the phenotypic change in PASMC. However, the underlying molecular mechanisms by which NFAT proteins regulate the PASMC phenotype still require further investigation.

Taken together, our results have unraveled a novel role of miR-124 in repressing NFAT activity by targeting multiple molecules (NFATc1, PTBP1, and CAMTA1), providing an important lead for the development of miRNA-based gene therapy. The down-regulation of miR-124 in both hypoxia-treated HPASMC and hypoxia-induced PAH mouse lungs and its ability to induce potent antiproliferative and prodifferentiation effects suggest that it may be of potential value for the treatment of PAH via the delivery of miR-124 mimic.

Acknowledgment—We thank Dr. Sekhar Reddy for critical reading of the manuscript.

REFERENCES

1. Shaw, J. P., Utz, P. J., Durand, D. B., Toole, J. J., Emmel, E. A., and Crabtree, G. R. (1988) Identification of a putative regulator of early T cell activation genes. *Science* **241,** 202–205
2. Hogan, P. G., Chen, L., Nardone, J., and Rao, A. (2003) Transcriptional regulation by calcium, calcineurin, and NFAT. *Genes Dev.* **17,** 2205–2232
3. Macian, F. (2005) NFAT proteins. Key regulators of T-cell development and function. *Nat. Rev. Immunol.* **5,** 472–484
4. Müller, M. R., and Rao, A. (2010) NFAT, immunity and cancer. A transcription factor comes of age. *Nat. Rev. Immunol.* **10,** 645–656
5. Archer, S. L., Weir, E. K., and Wilkins, M. R. (2010) Basic science of pulmonary arterial hypertension for clinicians. New concepts and experimental therapies. *Circulation* **121,** 2045–2066
6. Badesch, D. B., Champion, H. C., Sanchez, M. A., Hoeper, M. M., Loyd, J. E., Manes, A., McGoon, M., Naeije, R., Olschewski, H., Oudiz, R. J., and Torbicki, A. (2009) Diagnosis and assessment of pulmonary arterial hypertension. *J. Am. Coll. Cardiol.* **54,** S55–S66
7. Rubin, L. J. (2006) Pulmonary arterial hypertension. *Proc. Am. Thorac. Soc.* **3,** 111–115
8. Humbert, M., Morrell, N. W., Archer, S. L., Stenmark, K. R., MacLean, M. R., Lang, I. M., Christman, B. W., Weir, E. K., Eickelberg, O., Voelkel, N. F., and Rabinovitch, M. (2004) Cellular and molecular pathobiology of pulmonary arterial hypertension. *J. Am. Coll. Cardiol.* **43,** 13S–24S
9. Lagna, G., Ku, M. M., Nguyen, P. H., Neuman, N. A., Davis, B. N., and Hata, A. (2007) Control of phenotypic plasticity of smooth muscle cells by bone morphogenetic protein signaling through the myocardin-related transcription factors. *J. Biol. Chem.* **282,** 37244–37255
10. Bonnet, S., Rochefort, G., Sutendra, G., Archer, S. L., Haromy, A., Webster, L., Hashimoto, K., Bonnet, S. N., and Michelakis, E. D. (2007) The nuclear factor of activated T cells in pulmonary arterial hypertension can be therapeutically targeted. *Proc. Natl. Acad. Sci. U.S.A.* **104,** 11418–11423
11. Bierer, R., Nitta, C. H., Friedman, J., Codianni, S., de Frutos, S., Dominguez-Bautista, J. A., Howard, T. A., Resta, T. C., and Bosc, L. V. (2011) NFATc3 is required for chronic hypoxia-induced pulmonary hypertension in adult and neonatal mice. *Am. J. Physiol. Lung Cell Mol. Physiol.* **301,** L872–L880
12. de Frutos, S., Spangler, R., Alò, D., and Bosc, L. V. (2007) NFATc3 mediates chronic hypoxia-induced pulmonary arterial remodeling with α-actin up-regulation. *J. Biol. Chem.* **282,** 15081–15089
13. Hassoun, P. M., Mouthon, L., Barberà, J. A., Eddahibi, S., Flores, S. C., Grimminger, F., Jones, P. L., Maitland, M. L., Michelakis, E. D., Morrell, N. W., Newman, J. H., Rabinovitch, M., Schermuly, R., Stenmark, K. R., Voelkel, N. F., Yuan, J. X., and Humbert, M. (2009) Inflammation, growth factors, and pulmonary vascular remodeling. *J. Am. Coll. Cardiol.* **54,** S10–S19
14. Wang, C., Li, J. F., Zhao, L., Liu, J., Wan, J., Wang, Y. X., and Wang, J. (2009) Inhibition of SOC/Ca^{2+}/NFAT pathway is involved in the anti-proliferative effect of sildenafil on pulmonary artery smooth muscle cells. *Respir. Res.* **10,** 123
15. Huntzinger, E., and Izaurralde, E. (2011) Gene silencing by microRNAs. Contributions of translational repression and mRNA decay. *Nat. Rev. Genet.* **12,** 99–110
16. Lewis, B. P., Burge, C. B., and Bartel, D. P. (2005) Conserved seed pairing, often flanked by adenosines, indicates that thousands of human genes are microRNA targets. *Cell* **120,** 15–20

17. Cordes, K. R., Sheehy, N. T., White, M. P., Berry, E. C., Morton, S. U., Muth, A. N., Lee, T. H., Miano, J. M., Ivey, K. N., and Srivastava, D. (2009) miR-145 and miR-143 regulate smooth muscle cell fate and plasticity. *Nature* **460,** 705–710
18. Rangrez, A. Y., Massy, Z. A., Metzinger-Le Meuth, V., and Metzinger, L. (2011) miR-143 and miR-145. Molecular keys to switch the phenotype of vascular smooth muscle cells. *Circ. Cardiovasc. Genet.* **4,** 197–205
19. Xin, M., Small, E. M., Sutherland, L. B., Qi, X., McAnally, J., Plato, C. F., Richardson, J. A., Bassel-Duby, R., and Olson, E. N. (2009) MicroRNAs miR-143 and miR-145 modulate cytoskeletal dynamics and responsiveness of smooth muscle cells to injury. *Genes Dev.* **23,** 2166–2178
20. Courboulin, A., Paulin, R., Giguère, N. J., Saksouk, N., Perreault, T., Meloche, J., Paquet, E. R., Biardel, S., Provencher, S., Côté, J., Simard, M. J., and Bonnet, S. (2011) Role for miR-204 in human pulmonary arterial hypertension. *J. Exp. Med.* **208,** 535–548
21. Sarkar, J., Gou, D., Turaka, P., Viktorova, E., Ramchandran, R., and Raj, J. U. (2010) MicroRNA-21 plays a role in hypoxia-mediated pulmonary artery smooth muscle cell proliferation and migration. *Am. J. Physiol. Lung Cell Mol. Physiol.* **299,** L861–L871
22. Gou, D., Ramchandran, R., Peng, X., Yao, L., Kang, K., Sarkar, J., Wang, Z., Zhou, G., Zhou, G., and Raj, J. U. (2012) miR-210 has an antiapoptotic effect in pulmonary artery smooth muscle cells during hypoxia. *Am. J. Physiol. Lung Cell Mol. Physiol.* **303,** L682–L691
23. Li, Q., Lin, X., Yang, X., and Chang, J. (2010) NFATc4 is negatively regulated in miR-133a-mediated cardiomyocyte hypertrophic repression. *Am. J. Physiol. Heart Circ. Physiol.* **298,** H1340–H1347
24. Lin, Z., Murtaza, I., Wang, K., Jiao, J., Gao, J., and Li, P. F. (2009) miR-23a functions downstream of NFATc3 to regulate cardiac hypertrophy. *Proc. Natl. Acad. Sci. U.S.A.* **106,** 12103–12108
25. Wang, K., Long, B., Zhou, J., and Li, P. F. (2010) miR-9 and NFATc3 regulate myocardin in cardiac hypertrophy. *J. Biol. Chem.* **285,** 11903–11912
26. Gou, D., Weng, T., Wang, Y., Wang, Z., Zhang, H., Gao, L., Chen, Z., Wang, P., and Liu, L. (2007) A novel approach for the construction of multiple shRNA expression vectors. *J. Gene Med.* **9,** 751–763
27. Kang, K., Zhang, X., Liu, H., Wang, Z., Zhong, J., Huang, Z., Peng, X., Zeng, Y., Wang, Y., Yang, Y., Luo, J., and Gou, D. (2012) A novel real-time PCR assay of microRNAs using S-Poly(T), a specific oligo(dT) reverse transcription primer with excellent sensitivity and specificity. *PLoS One* **7,** e48536
28. Willingham, A. T., Orth, A. P., Batalov, S., Peters, E. C., Wen, B. G., Aza-Blanc, P., Hogenesch, J. B., and Schultz, P. G. (2005) A strategy for probing the function of noncoding RNAs finds a repressor of NFAT. *Science* **309,** 1570–1573
29. Kozomara, A., and Griffiths-Jones, S. (2011) miRBase. Integrating microRNA annotation and deep-sequencing data. *Nucleic Acids Res.* **39,** D152–D157
30. Bartel, D. P. (2009) MicroRNAs. Target recognition and regulatory functions. *Cell* **136,** 215–233
31. Voorhoeve, P. M., le Sage, C., Schrier, M., Gillis, A. J., Stoop, H., Nagel, R., Liu, Y. P., van Duijse, J., Drost, J., Griekspoor, A., Zlotorynski, E., Yabuta, N., De Vita, G., Nojima, H., Looijenga, L. H., and Agami, R. (2006) A genetic screen implicates miRNA-372 and miRNA-373 as oncogenes in testicular germ cell tumors. *Cell* **124,** 1169–1181
32. Weitzel, R. P., Lesniewski, M. L., Haviernik, P., Kadereit, S., Leahy, P., Greco, N. J., and Laughlin, M. J. (2009) microRNA 184 regulates expression of NFAT1 in umbilical cord blood CD4+ T cells. *Blood* **113,** 6648–6657
33. Arron, J. R., Winslow, M. M., Polleri, A., Chang, C. P., Wu, H., Gao, X., Neilson, J. R., Chen, L., Heit, J. J., Kim, S. K., Yamasaki, N., Miyakawa, T., Francke, U., Graef, I. A., and Crabtree, G. R. (2006) NFAT dysregulation by increased dosage of DSCR1 and DYRK1A on chromosome 21. *Nature* **441,** 595–600
34. Ikeda, S., He, A., Kong, S. W., Lu, J., Bejar, R., Bodyak, N., Lee, K. H., Ma, Q., Kang, P. M., Golub, T. R., and Pu, W. T. (2009) MicroRNA-1 negatively regulates expression of the hypertrophy-associated calmodulin and Mef2a genes. *Mol. Cell Biol.* **29,** 2193–2204
35. Agirre, X., Vilas-Zornoza, A., Jiménez-Velasco, A., Martin-Subero, J. I., Cordeu, L., Gárate, L., San José-Eneriz, E., Abizanda, G., Rodríguez-Otero, P., Fortes, P., Rifón, J., Bandrés, E., Calasanz, M. J., Martín, V., Heiniger, A., Torres, A., Siebert, R., Román-Gomez, J., and Prósper, F. (2009) Epigenetic silencing of the tumor suppressor microRNA Hsa-miR-124a regulates CDK6 expression and confers a poor prognosis in acute lymphoblastic leukemia. *Cancer Res.* **69,** 4443–4453
36. Lim, L. P., Lau, N. C., Garrett-Engele, P., Grimson, A., Schelter, J. M., Castle, J., Bartel, D. P., Linsley, P. S., and Johnson, J. M. (2005) Microarray analysis shows that some microRNAs downregulate large numbers of target mRNAs. *Nature* **433,** 769–773
37. Lindenblatt, C., Schulze-Osthoff, K., and Totzke, G. (2009) IκBζ expression is regulated by miR-124a. *Cell Cycle* **8,** 2019–2023
38. Sanuki, R., Onishi, A., Koike, C., Muramatsu, R., Watanabe, S., Muranishi, Y., Irie, S., Uneo, S., Koyasu, T., Matsui, R., Chérasse, Y., Urade, Y., Watanabe, D., Kondo, M., Yamashita, T., and Furukawa, T. (2011) miR-124a is required for hippocampal axogenesis and retinal cone survival through Lhx2 suppression. *Nat. Neurosci.* **14,** 1125–1134
39. Venkatesh, N., Feng, Y., DeDecker, B., Yacono, P., Golan, D., Mitchison, T., and McKeon, F. (2004) Chemical genetics to identify NFAT inhibitors. Potential of targeting calcium mobilization in immunosuppression. *Proc. Natl. Acad. Sci. U.S.A.* **101,** 8969–8974
40. Makeyev, E. V., Zhang, J., Carrasco, M. A., and Maniatis, T. (2007) The MicroRNA miR-124 promotes neuronal differentiation by triggering brain-specific alternative pre-mRNA splicing. *Mol. Cell* **27,** 435–448
41. Smith, P., Al Hashimi, A., Girard, J., Delay, C., and Hébert, S. S. (2011) *In vivo* regulation of amyloid precursor protein neuronal splicing by microRNAs. *J. Neurochem.* **116,** 240–247
42. Henrich, K. O., Bauer, T., Schulte, J., Ehemann, V., Deubzer, H., Gogolin, S., Muth, D., Fischer, M., Benner, A., König, R., Schwab, M., and Westermann, F. (2011) CAMTA1, a 1p36 tumor suppressor candidate, inhibits growth and activates differentiation programs in neuroblastoma cells. *Cancer Res.* **71,** 3142–3151
43. Finkler, A., Ashery-Padan, R., and Fromm, H. (2007) CAMTAs. Calmodulin-binding transcription activators from plants to human. *FEBS Lett.* **581,** 3893–3898
44. Pierson, J., Hostager, B., Fan, R., and Vibhakar, R. (2008) Regulation of cyclin dependent kinase 6 by microRNA 124 in medulloblastoma. *J. Neurooncol.* **90,** 1–7
45. Baroukh, N. N., and Van Obberghen, E. (2009) Function of microRNA-375 and microRNA-124a in pancreas and brain. *FEBS J.* **276,** 6509–6521
46. Cheng, L. C., Pastrana, E., Tavazoie, M., and Doetsch, F. (2009) miR-124 regulates adult neurogenesis in the subventricular zone stem cell niche. *Nat. Neurosci.* **12,** 399–408
47. Baroukh, N., Ravier, M. A., Loder, M. K., Hill, E. V., Bounacer, A., Scharfmann, R., Rutter, G. A., and Van Obberghen, E. (2007) MicroRNA-124a regulates Foxa2 expression and intracellular signaling in pancreatic beta-cell lines. *J. Biol. Chem.* **282,** 19575–19588
48. Laine, S. K., Alm, J. J., Virtanen, S. P., Aro, H. T., and Laitala-Leinonen, T. K. (2012) MicroRNAs miR-96, miR-124, and miR-199a regulate gene expression in human bone marrow-derived mesenchymal stem cells. *J. Cell Biochem.* **113,** 2687–2695
49. Catuogno, S., Cerchia, L., Romano, G., Pognonec, P., Condorelli, G., and de Franciscis, V. (2013) miR-34c may protect lung cancer cells from paclitaxel-induced apoptosis. *Oncogene* **32,** 341–351
50. Owens, G. K., Kumar, M. S., and Wamhoff, B. R. (2004) Molecular regulation of vascular smooth muscle cell differentiation in development and disease. *Physiol. Rev.* **84,** 767–801
51. Yoo, A. S., Staahl, B. T., Chen, L., and Crabtree, G. R. (2009) MicroRNA-mediated switching of chromatin-remodelling complexes in neural development. *Nature* **460,** 642–646
52. Silber, J., Lim, D. A., Petritsch, C., Persson, A. I., Maunakea, A. K., Yu, M., Vandenberg, S. R., Ginzinger, D. G., James, C. D., Costello, J. F., Bergers, G., Weiss, W. A., Alvarez-Buylla, A., and Hodgson, J. G. (2008) miR-124 and miR-137 inhibit proliferation of glioblastoma multiforme cells and induce differentiation of brain tumor stem cells. *BMC Med.* **6,** 14
53. Krichevsky, A. M., Sonntag, K. C., Isacson, O., and Kosik, K. S. (2006) Specific microRNAs modulate embryonic stem cell-derived neurogenesis. *Stem Cells* **24,** 857–864

54. Thompson, J., Lepikhova, T., Teixido-Travesa, N., Whitehead, M. A., Palvimo, J. J., Jänne, O. A. (2006) Small carboxyl-terminal domain phosphatase 2 attenuates androgen-dependent transcription. *EMBO J.* **25,** 2757–2767
55. Cho, S., Kim, J. H., Back, S. H., and Jang, S. K. (2005) Polypyrimidine tract-binding protein enhances the internal ribosomal entry site-dependent translation of p27Kip1 mRNA and modulates transition from G_1 to S phase. *Mol. Cell. Biol.* **25,** 1283–1297
56. Nde, P. N., Simmons, K. J., Kleshchenko, Y. Y., Pratap, S., Lima, M. F., and Villalta, F. (2006) Silencing of the laminin γ-1 gene blocks *Trypanosoma cruzi* infection. *Infect. Immun.* **74,** 1643–1648
57. Qiao, L., MacLean, P. S., You, H., Schaack, J., and Shao, J. (2006) Knocking down liver CCAAT/enhancer-binding protein α by adenovirus-transduced silent interfering ribonucleic acid improves hepatic gluconeogenesis and lipid homeostasis in db/db mice. *Endocrinology* **147,** 3060–3069
58. Martin, S. E., Jones, T. L., Thomas, C. L., Lorenzi, P. L., Nguyen, D. A., Runfola, T., Gunsior, M., Weinstein, J. N., Goldsmith, P. K., Lader, E., Huppi, K., and Caplen, N. J. (2007) Multiplexing siRNAs to compress RNAi-based screen size in human cells. *Nucleic Acids Res.* **35,** e57
59. Franco, M., Furstoss, O., Simon, V., Benistant, C., Hong, W. J., and Roche, S. (2006) The adaptor protein Tom1L1 is a negative regulator of Src mitogenic signaling induced by growth factors. *Mol. Cell Biol.* **26,** 1932–1947
60. Di Sole, F., Cerull, R., Babich, V., Quiñones, H., Gisler, S. M., Biber, J., Murer, H., Burckhardt, G., Helmle-Kolb, C., and Moe, O. W. (2004) Acute regulation of Na/H exchanger NHE3 by adenosine A(1) receptors is mediated by calcineurin homologous protein. *J. Biol. Chem.* **279,** 2962–2974